HHS Public Access

Author manuscript

Min Metall Explor. Author manuscript; available in PMC 2019 August 01.

Published in final edited form as:

Min Metall Explor. 2019 August ; 36(4): 729–740. doi:10.1007/s42461-019-0065-7.

Investigating the Impact of Caving on Longwall Mine Ventilation Using Scaled Physical Modeling

V. Gangrade[1], **S. J. Schatzel**[1], **S. P. Harteis**[1], **J. D. Addis**[1]

[1]National Institute for Occupational Safety and Health (NIOSH), 626 Cochrans Mills Rd, Pittsburgh, PA 15236, USA

Abstract

In longwall mining, ventilation is considered one of the more effective means for controlling gases and dust. In order to study longwall ventilation in a controlled environment, researchers built a unique physical model called the Longwall Instrumented Aerodynamic Model (LIAM) in a laboratory at the National Institute for Occupational Safety and Health (NIOSH) Pittsburgh Mining Research Division (PMRD) campus. LIAM is a 1:30 scale physical model geometrically designed to simulate a single longwall panel with a three-entry headgate and tailgate configuration, along with three back bleeder entries. It consists of a two-part heterogeneous gob that simulates a less compacted unconsolidated zone and more compacted consolidated zone. It has a footprint of 8.94 m (29 ft.) by 4.88 m (16 ft.), with a simulated face length of 220 m (720 ft.) in full scale. LIAM is built with critical details of the face, gob, and mining machinery. It is instrumented with pressure gauges, flow anemometers, temperature probes, a fan, and a data acquisition system. Scaling relationships are derived on the basis of Reynolds and Richardson numbers to preserve the physical and dynamic similitude. This paper discusses the findings from a study conducted in the LIAM to investigate the gob-face interaction, airflow patterns within the gob, and airflow dynamics on the face for varying roof caving characteristics. Results are discussed to show the impact of caving behind the shields on longwall ventilation.

Keywords

Mine ventilation; Longwall mining; Roof caving; Physical modeling

1 Introduction

Ventilation is an important means of controlling gases and dusts in underground mines, and is critical to maintaining the safety and health of the underground workforce. Explosive methane gas is released during the mining process and can accumulate in areas that are not well ventilated. Historically, most methane-related mining explosion disasters originated at

V. Gangrade VGangrade@cdc.gov.

Compliance with Ethical Standards

Disclaimer The findings and conclusions in this paper are those of the authors and do not necessarily represent the views of the National Institute for Occupational Safety and Health, Centers for Disease Control and Prevention. Mention of any company or product does not constitute endorsement by NIOSH.

Conflict of Interest The authors declare that they have no conflict of interest.

or near the active production or development faces. Longwall mining presents a particularly unique situation where not only are large quantities of methane gas liberated but large methane reservoirs are created concurrently. Given the risk of methane accumulations on longwall faces, ventilation of such systems must be constantly maintained. Therefore, designing and maintaining an efficient ventilation system for a longwall mine is of utmost importance for mine operators.

The extent of roof caving behind the shields is an important consideration for maintaining adequate longwall face ventilation. The roof rock over the mined coal seam can range from brittle to very strong and competent. If the rock is brittle, the material can cave tightly behind the longwall shields as mining proceeds. In the case of very strong roof, the roof may not immediately cave, leaving a significant void space extending into the mined-out area (gob). Although the literature is replete with published work on ground control aspects of the roof caving characteristics [1–4], the effect of caving characteristics on longwall mine ventilation is not well known. Air exchanges between the face area and gob of a longwall operation have been documented by a number of researchers for different ventilation systems in several mines; however, there is no substantial data available on the caving characteristics and their impact on the ventilation systems.

Researchers and engineers around the world have always found new and innovative research approaches to investigate mine ventilation systems. Currently, three main research methods are used to improve the understanding of ventilation in longwall mines: numerical modeling, field studies, and physical modeling. Numerical modeling studies have primarily been conducted using the computational fluid dynamics modeling (CFD) [5–12] and ventilation network simulators [13, 14]. CFD provides the advantage to model fluid flow and estimate gas concentration in inaccessible areas of the longwall mines, such as gobs. Ventilation network simulators provide the advantage of solving the overall pressure or airflow distribution in the entire mine ventilation system but are limited in ability to provide airflow distribution in different cross-sections. Researchers have also used advanced fracture modeling using discrete fracture network (DFN) based on random and discrete nature of fractures in the longwall gob and multidimensional reservoir modeling [15–17]. Field studies are one the most effective and accurate way to investigate longwall ventilation; investigations have been conducted using a variety of research approaches including tracer gas studies, atmospheric monitoring, and ventilation surveys [18–20]. Physical modeling research approach is widely used in aeronautic, automobile, construction, and defense industries, but there have been few investigations to investigate mine ventilation systems. Jones and Lowrie made significant efforts to develop a ½0th and 1/70th scale physical model to simulate 100-m and 200-m sections of longwall face, respectively [21, 22]. Gangrade et al. developed 1/30th scale model of a mine section to investigate application of booster fans in coal mines [23]. Calizaya et al. used a scaled coal mine model to investigate the application of pressure balancing techniques to control spontaneous combustion [24]. Pan et al. developed a 1/100th scale physical model to investigate the gas dilution in a block-caving mine [25]. Fig et al. used a scaled cylindrical tube to investigate the methane ignition and flame propagation to describe methane-driven longwall coal mine explosions [26].

Researchers with the National Institute for Occupational Safety and Health (NIOSH) Pittsburgh Mining Research Division (PMRD) employed a physical modeling approach to study the potential impact of gob void space on longwall face ventilation. The complex and dynamic nature of longwall mining makes it difficult to conduct detailed field experiments for different caving conditions in a particular mine. As an alternative, physical modeling can be used to simulate areas of a longwall panel that are inaccessible. Scaled physical modeling also offers the advantage of simulating the performance of a ventilation system under controlled conditions. For this purpose, a 1:30 scale physical model of a portion of a longwall operation was designed and constructed. The Longwall Instrumented Aerodynamic Model (LIAM) is built with critical details of the face and face machinery, including a shearer, shields, and pan-line, as well as a portion of the gob and the barrier pillars (Fig. 1). LIAM is constructed to simulate ventilation flow in a controlled environment, allowing variables to be systematically modified [27, 28].

Bleeder and bleederless systems were simulated with a range of void spaces behind the shields. In the context of this paper, caving to the shields when the face moves forward is considered to be the normal caving scenario. Airflow pathways at the tailgate corner were investigated, and locations of potential gob-face interaction were identified.

2 Longwall Instrumented Aerodynamic Model (LIAM)

The 1:30-scale LIAM was designed to maintain similitude with the main properties of flow in full scale. The important characteristics of the model are described as follows.

2.1 Model Design

LIAM is geometrically designed to represent a single longwall panel with a three-entry headgate and a three-entry tailgate configuration. It also has three back bleeder entries (Figs. 1 and 2). It has a footprint of 8.94 m (29 ft.) length by 4.88 m (16 ft.) width and is 0.84 m (2.75 ft.) in height from the floor to the surface of the model. LIAM's mine entries and crosscuts are 19.3 cm (7.60 in.) on average, which simulates a 5.79-m (19-ft.) entry width in full scale. The longwall face length in LIAM is 7.31 m (24 ft.), which represents a 219.5-m (720-ft.) longwall face in full scale. A 3-D printer was used to create the model longwall shearer with cutting drums. The shearer, coal face, and shield placement simulate coal cutting from the headgate side towards the tailgate side.

The top surface of LIAM is protected by 0.95-cm (0.38-in.) clear acrylic glass. The transparent acrylic glass allows a clear view inside the model and visualization of airflow in the model using smoke. The smoke is created using a theatrical smoke generator. Smoke helps in observing and validating the flow paths, eddy currents, turbulence, and gob-face interaction.

2.2 Gob

The gob in the LIAM simulates the typical caving characteristics in a longwall mine, representing consolidated and unconsolidated zones. Two types of gob materials were used to simulate the different porosities of the gob: broken pieces of Styrofoam (52% porous) to simulate a less compacted unconsolidated zone behind the shields and gravel (33% porous)

to simulate the more compacted consolidated zone in the gob. The extent of gob represents an early stage of mining before the gob is “squared up”— i.e., where the length of the gob equals the face width. In its current configuration, LIAM is not set up to model the vertical extent of roof caving above the mined seam.

2.3 Ventilation

The LIAM uses one fan which can be connected to either the headgate, tailgate, or bleeder exhaust to simulate different ventilation configurations. In addition, there are four regulators within the model to redirect air to different entries (Fig. 1). The fan selected for LIAM is a regenerative blower centrifugal fan, 480 VAC, 930 W, connected to a variable frequency drive.

2.4 Instrumentation

A number of parameters are monitored in LIAM. To measure ventilation flow rates, 13 hotwire anemometers are located in different areas of the model: 8 anemometers on the face and 32 anemometers within the gob. The hotwire anemometers were calibrated against a vane anemometer before installation. Pressure differential across the face is measured using pressure transducers—one at the headgate and one at the tailgate of the face. Two thermocouples are used to measure the temperature of air in the model and in the building where LIAM is located. The locations of different sensors are shown in Fig. 2. The data acquisition system selected for this study is Measurement Computing/Data Translations Inc.’s MEASURpoint hardware with QuickDAQ software [29]. It has eight thermocouple cold junction compensated channels and 32 voltage channels (±10 V). All channels are fully isolated, with ± 500-V galvanic isolation channel-to-channel and earth-to-earth ground. An LCD monitor directly connected to the data acquisition system is installed in the building to show sensor data in real time.

3 Scaling Factors

The concept of scaling using physical models has been applied widely in industrial and environmental fluid flow studies. In mining, however, the complex and dynamic nature of an underground mine has made modeling studies more complicated and difficult for investigation of ventilation problems. The validity of any scaled model depends on a set of similarity relationships between important physical properties of flow in the model compared with the flow in full scale. Therefore, it is important to obtain similar flow characteristics in the model and in full scale in relation to buoyancy, dispersion of layers, and molecular diffusion. The main sources of information for developing the principles of scaling the flow are the studies done by Jones and Lowrie [21, 22] and Aitken et al. [30]. The classical analysis of turbulent dispersion by Taylor [31] helps provide a basis for using different scaling factors for velocity and geometry—thus allowing the maximum reduction of geometric scale to be achieved. For aerodynamic scaling of LIAM, optimal similitude could be achieved between the model and full scale if a number of conditions are met. These conditions include (1) the Reynolds number for airflow on the face being kept greater than 6000 to develop turbulent flow and (2) the conservation of the Richardson number to

preserve the layer dispersion properties [32]. Equations 1 and 2 represent the aerodynamic scaling of airflow in LIAM.

$$\text{Reynolds number, } Re = \frac{\rho V L}{\mu} \quad (1)$$

where ρ is the density, V is the characteristic velocity, μ is the dynamic viscosity of the fluid, and L is the characteristic linear dimension.

$$\text{Richardson number, } Ri = g\frac{\Delta\rho \times d}{\rho_a \times v^2} \quad (2)$$

where g is the gravity, $\Delta\rho$ is the density difference between the air and methane, d is the characteristic length scale, ρ_a is the density of air, and v is the bulk velocity.

Table 1 summarizes the scaling factors for the design and operation of LIAM, so that the flows are dynamically similar to the flows in full scale.

While determining the scaling factors for geometry and velocity, consideration was also given to future experiments that will be conducted for simulating gas emission in the gob.

4 Experimental Tests

Experimental tests were conducted in LIAM to measure the air velocities within the gob and to determine the gob-face interaction and movement of air for longwall panels with different roof caving characteristics. The study was conducted on a single longwall panel with a three-entry headgate and a three-entry tailgate configuration (Fig. 2). Bleeder and bleederless ventilation systems were tested for different caving characteristics. For the bleeder system, the bleeder exhaust on the tailgate side was used to simulate the bleeder shaft. For the bleederless system, stoppings were added around the gob. Between the gob and back entries, one crosscut was left open on the tailgate side to represent the common practice in the US coal mines (Fig. 2).

Four caving scenarios were simulated: (1) no void space behind the shields, (2) 6-in. void space (simulates 4.57 m/15 ft. in full scale), (3) 12-in. of void space (simulates 9.14 m/30 ft. in full scale), and (4) a rarer scenario with 18 in. of void space (simulating 13.7 m/ 45 ft. in full scale). The four caving scenarios are shown in Fig. 3. The ventilation was initially set up for the normal caving condition. In the context of this paper, caving to the shields when the face moves forward is considered to be the normal caving scenario. The ventilation settings such as fan rpm and regulator opening were kept similar for the four scenarios, with the same amount of air at the headgate side of the face. This allowed for comparison of the impact of caving on ventilation in each case. Each test was conducted for 15 min with the sensor data being recorded at a frequency of 1 Hz. The sensor data was exported to Microsoft Excel for statistical analysis. Each test was repeated three times to ensure data reproducibility and minimize experimental error.

5 Results

Figures 4, 5, 6, and 7 show the results from the four caving scenarios discussed above. For simplicity and legibility, only airflow patterns in the gob and airflow readings on the face are shown in these figures. However, during the actual test, other parameters such as air velocities in the face, gob and entries, temperature, and pressure differential were also recorded. For each caving scenario, both bleeder and bleederless configurations were simulated.

5.1 Caving Scenario 1: No Void Space Behind the Shields

Results for the no void space caving scenario are shown in Fig. 4. This scenario is representative of a longwall mine where the roof in the gob caves right up to the shields as the face retreats further. To simulate this scenario, the gob was completely filled with gravel (consolidated zone) and Styrofoam (unconsolidated zone) to the shield canopies without leaving any open void space. For the bleeder configuration, most of the air traveled along the length of the face from the headgate side to the tailgate side, with some air traveling behind the shield line. The differential pressure across the face in the LIAM was 151 Pa (0.61 in.w.g.). On the face, part of the air entered the gob in front of the shearer (choosing the path of least resistance) and came back on the face inby the shearer. For the flow in the gob, it was observed that air entered the shield legs on the headgate side of the face and traveled from the front of the gob towards the back bleeder entries. Hotwire anemometers in the gob were able to record the air velocities within a range of 0.025–2.54 m/s (5–500 fpm). Since the cross-sectional areas are not well defined around the sensors in the gob, the airflow quantities were not calculated. Differential pressure was measured across the longwall face.

Flows through the gob were compared for different scenarios using the air velocities. As expected, the air velocities were higher in the less compacted unconsolidated zone compared with the more compacted consolidated zone within the gob. Airflow through the high permeability region moved generally from headgate to tailgate side, roughly paralleling face airflow.

For the bleederless configuration, seals were added around the gob and the back bleeder exhaust was closed. To make sure that the bleeder and bleederless configurations were comparable with each other, similar intake airflows were maintained. Ventilation air traveled along the length of the face from the headgate to the tailgate. The differential pressure across the face in the LIAM was 152 Pa (0.61 in.w.g.). Overall, there was more air at every location on the face for the bleederless system compared with the bleeder system, as shown in Fig. 4. Similar to the bleeder system, a portion of air traveled behind the shield line. However, both the data and smoke visualization showed that, in this case, some air came back on the face near the midface region. A similar phenomenon of more than one pathway of air and movement from the gob to the face has also been seen in a recent field study conducted by the authors [20]. Such movement of air in the gob’s void space may have severe mine safety implications, as the coalbed methane can get mixed with air and come back on the face on the tailgate side.

The back of the gob is sealed for the bleederless system; therefore, air travels almost parallel to the face from the headgate to the tailgate side. Similar to the bleeder system, the air velocities in the less compacted unconsolidated zone were higher than those in the more compacted consolidated zone of the gob, with flow being in a general headgate to tailgate direction. Air velocities in the gob for the bleederless system were slightly lower in this case compared with those for the bleeder system. The quantity of airflow could not be accurately determined within the gob.

5.2 Caving Scenario 2: 4.57-m (15-Ft.) Void Space Behind the Shields

Figure 5 shows the results from the scenario simulating 4.57 m (15 ft.) of void space behind the shields. Such roof caving characteristics are observed in longwall mines where the roof does not cave immediately once the face retreats further. This scenario also holds true for the early stages of a longwall panel, when the face begins to retreat and the roof does not immediately cave due to the support from pillars in the back of the gob, leaving a void space behind the shields. For both the bleeder and bleederless systems, the airflow on the face was the same order of magnitude. However, the flow on the face decreased compared with that observed with no void space. The differential pressure across the face for the bleeder system was 144 Pa (0.58 in.w.g.) and for the bleederless system was 152 Pa (0.61 in.w.g.). In this situation, ventilation air traveled through the void behind the shield line at a very high velocity. For the bleeder scenario, an air velocity as high as 0.60 m/s (118 fpm) was recorded in the gob opposite the shearer. For the bleederless scenario, an air velocity as high as 0.85 m/s (167 fpm) was recorded in a similar location. Higher air velocities were measured at other locations in the open gob for both configurations. Such movement of air in the gob's void space may have severe mine safety implications, as the coalbed methane can get mixed with air and come back on the face on the tailgate side.

Air velocities in the consolidated zone were lower than those in the unconsolidated zone of the gob. Paths between the unconsolidated zone of the gob material were clearly visible using the theatrical smoke (Fig. 1), while velocities recorded were near or below the sensor limit (<0.025 m/s). In the gob, the ventilation flow was moving from the front of the gob towards the back of the gob for the bleeder system and parallel to the face for the bleederless system.

5.3 Caving Scenario 3: 9.14-m (30-ft.) Void Space Behind the Shields

Figure 6 shows the results from the tests simulating 9.14 m (30 ft.) of void space behind the shields. This roof caving scenario may occur in mines with a highly competent roof that does not cave as the face retreats. Some western mines in the USA have such conditions due to the presence of a highly competent roof. In this scenario, the flow rates on the face decreased further compared with scenarios 1 and 2. The flow on the face was very slow, especially on the tailgate side. This occurred because a major portion of the air on the face entered the gob through the shield legs (as shown in Fig. 6). The large void space behind the shields provided a path of least resistance to the airflow on the headgate side of the face. The highest air velocities measured behind the shields were 0.31–0.41 m/s (60–80 fpm) for the bleeder system, which was lower than seen for the 4.57-m (15-ft.) void condition. Similarly, the highest air velocity behind the shield line for the bleederless system was 0.61 m/s (120

fpm), which was lower than the value of 0.81 m/s (160 fpm) for the 4.57-m (15-ft.) void condition. Only a very small portion of ventilation air was traveling in the consolidated and unconsolidated zones of the gob in this scenario. The differential pressure across the face for the bleeder system was 157 Pa (0.63 in.w.g.) and for the bleederless system was 173 Pa (0.70 in.w.g.)

5.4 Caving Scenario 4:13.7-m (45-ft.) Void Space Behind the Shields

Figure 7 shows the results from the tests simulating 13.7 m (45 ft.) of void space behind the shields. Such roof caving conditions are rare in US longwall mines and only occur when the roof is very competent. In this scenario, the large void space had a large impact on the longwall ventilation. In both the bleeder and bleederless configurations, there was a high degree of air recirculation and eddy formation in the gob near the headgate side. Air entered the shield legs on headgate side and recirculated with very high velocity before moving towards the tailgate. On the face, the air was moving from the face and into the gob for almost ¾ of the face length. Due to this loss of air to the gob, more than half the face length could not be ventilated properly; this can have severe consequence for longwall operation during cutting of coal. Within the gob, the air velocities and patterns for both the bleeder and bleederless configurations were similar to each other, with most of the air traveling from the headgate side towards the tailgate side in the large void space. Similar to the 9.14-m void space scenario, a very small portion of ventilation air was traveling in the consolidated and unconsolidated zones of the gob. The differential pressure across the face for the bleeder system was 161 Pa (0.65 in.w.g.) and for the bleederless system was 137 Pa (0.55 in.w.g.).

6 Discussion

Data from the air velocity sensors in the gob showed that, when void space increases, the differences between the air velocity contours in bleeder and bleederless ventilation systems decrease. The comparison plots in Fig. 8 are for bleeder and bleederless configurations for the 13.7-m (45-ft.) void space scenario. The upper plot is a contour map, and the lower plot is a 3-D surface map of the data from the gob. As shown in Fig. 8, even though the velocity numbers are slightly higher for the bleederless configuration, the overall pattern and contours are almost identical to each other. This phenomenon suggests that, if there is a large volume of void space behind the shields, it can be very difficult to ventilate the face with either ventilation system, in that air leakage from the face through the shields is pronounced and the void space creates a low-resistance pathway of flow that can potentially cause both gas and sponcom problems.

The data also suggest that, with greater void space behind the shields, the ventilation air loss at the tailgate increases. This finding can be seen in Fig. 9, where the blue boxes show the air velocities in the gob, the yellow boxes show the airflow on the face in LIAM, and the green boxes show the full-scale airflow on the face. Figure 9a is the no void space scenario, where there is an adequate amount of air on the face at all locations. However, when the void space increases to 9.14 m (30 ft.) (Fig. 9b), there is a much lower quantity of air on the face, especially on the tailgate side. Much higher velocities exist in front of the gob. The quantity of air on the headgate side was similar in both cases, but the quantity of air on the tailgate

side observed with a 9.14-m (30ft.) void space may be inadequate to ventilate the face safely. This suggests that greater void space behind shields can cause ventilation redirection from the face to the gob.

Figure 10 shows the airflow data on the tailgate side of the face for the different caving scenarios in a bleeder configuration. Eight air velocity sensors were located on the face from the headgate side towards the tailgate side; the sensor locations are also shown in Fig. 10 below the graph. The amount of air at the headgate is similar for each scenario. This graph shows that airflow decreases more at all locations when transitioning from no void space to a 4.57m void space, in comparison to transitioning from a 9.14-m to a 13.7-m void space. There was a general pattern of lower airflow on the face with increasing void space behind the shields. Similar patterns of airflow on the face were also observed by Peng and Chiang (1986) [33] in their research based on the data collected on four mechanized longwall coal faces. A similar pattern of air loss on the face with increasing void space was also observed for the bleederless configuration.

7 Summary

An aerodynamically and geometrically scaled physical model was successfully developed to conduct longwall ventilation experiments. Ventilation tests for bleeder and bleederless configurations were simulated for different caving scenarios. It was observed that increasing void space behind the shields led to lower quantity of airflow on the face and a higher quantity of airflow in the gob. For 4.57 m (15 ft.) of void space behind the shields, airflow decreased on the face for both bleeder and bleederless scenarios when compared with the no void space scenario. In addition, velocities as high as 0.60 m/s (118 fpm) were recorded in the gob for the bleeder scenario, and 0.85 m/s (167 fpm) for the bleederless scenario. For 9.14 m (30 ft.) of void space behind the shields, the airflow on the face decreased further, leading to very low air quantities on the tailgate side of the face. The air velocities recorded in the gob were 0.31–0.41 m/s (60–80 fpm) for the bleeder configuration and 0.61 m/s (120 fpm) for the bleederless configuration. In this scenario, only a small portion of air traveled in the less compacted (Styrofoam) region and more compacted (gravel) region. In the scenario with 13.7 m (45 ft.) of void space behind the shields, a major portion of the airflow moved into the gob from the face. In both the bleeder and bleederless configurations, there was degree of air recirculation and eddy formation in the gob. The results suggest that caving characteristics have a significant impact on the ventilation of a longwall panel.

In addition to the LIAM studies, a research team also investigated the important aspects of longwall ventilation using numerical modeling and field studies. Numerical modeling research utilized computational fluid dynamics modeling and discrete fracture network modeling concept [15]. Field studies were conducted at three longwall mines in the USA with different face lengths: 228 m, 305 m, and 381 m. Reports from two field studies have been published [18, 20]. Results from the LIAM studies are in agreement with the findings from companion research approaches. Future studies in the LIAM are planned to investigate gas emissions in a longwall panel. These studies will involve the use of tracer gas as a surrogate for methane and would improve the understanding of the movement of gas in a longwall panel.

References

1. Pappas D, Christopher M (1993) Behavior of simulated longwall gob material. Report of investigations, US Bureau of Mines
2. Esterhuizen E, Mark C, Murphy MM (2010) Numerical model calibration for simulating coal pillars, gob and overburden response. In: Proceedings - 29th International Conference on Ground Control in Mining, ICGCM 2010, pp 46–57
3. Zhang CTS, Zhao YX (2019) Compaction characteristics of the caving zone in a longwall goaf: a review. Environ Earth Sci 78(1):27
4. Zhang C, Yu L, Feng R, Zhang Y, Zhang G (2019) A numerical study of stress distribution and fracture development above a protective coal seam in longwall mining. Processes 6(9) art. no. 146
5. Brune JF, Sapko M (2012) A modeling study on longwall tailgate ventilation. In: Proceedings of the 14th Annual North American Ventilation Conference, 121–126. University of Utah, Salt Lake City, UT
6. Yuan L, Smith AC, Brune JF (2012) Computational fluid dynamics study on the ventilation flow paths in longwall gobs. In: Proceedings of the 11th U.S./North American Mine Ventilation Symposium, University Park, PA
7. Gilmore RC (2015) CFD modeling of underground coal longwall gob ventilation systems using a developed meshing approach. Dissertation, Colorado School of Mines
8. Mishra DP, Kumar P, Panigrahi DC (2016) Dispersion of methane in tailgate of a retreating longwall mine: a computational fluid dynamics study. Environ Earth Sci 75(6):Article number 475
9. Lolon SA, Brune JF, Bogin GE Jr, Grubb JW, Saki SA, Juganda A (2017) Computational fluid dynamics simulation on the longwall gob breathing. Int J Min Sci Technol 27(2):185–189
10. Juganda A, Brune J, Bogin G, Strebinger C, Fig M, Zurhorst M (2018) Incorporating ventilation network simulation into CFD modeling to analyze airflow distribution around longwall panels. 2018 SME Annual Conference and Expo and 91st Annual Meeting of the SME-MN Section, Volume 2018-February, 2018
11. Ren T, Wang Z, Liang Y, Zhang J (2018) Numerical investigation of CO2 fringe behaviour on a longwall face and its control. Int J Coal Geol 186:80–96
12. Wang Z, Ren T, Ma L, Zhang J (2018) Investigations of ventilation airflow characteristics on a longwall face—a computational approach. Energies 11:1564 10.3390/en11061564
13. Zhang Y, Zhang X, Habibi A, Tien JC (2012) Comparison of mine ventilation simulation software. 2012 SME Annual Meeting and Exhibit 2012, SME 2012, Meeting Preprints 2012, pp 670–674
14. Xu G, Huang J, Nie B, Chalmers D, Yang Z (2018) Calibration of mine ventilation network models using the non-linear optimization algorithm. Energies 11:31
15. Karacan CÖ, Yuan L (2015) Effect of discrete fracture network representation of gob on. Airflow distribution near the longwall face. In: Proceedings of the 15th North American Mine Ventilation Symposium, Blacksburg, VA
16. Ajayi K, Shahbazi K, Tukkaraja P, Katzenstein K (2019) Estimation of radon diffusivity tensor for fractured rocks in cave mines using a discrete fracture network model. J Environ Radioact 196:104–112 [PubMed: 30447553]
17. Karacan CO, Esterhuizen GS, Schatzel SJ, Diamond WP (2007) Reservoir simulation-based modeling for characterizing longwall methane emissions and gob gas venthole production. Int J Coal Geol 86:121–156
18. Schatzel SJ, Krog RB, Dougherty H (2017) Methane emissions and airflow patterns on a longwall face: potential influences from longwall gob permeability distributions on a bleederless longwall panel. Trans Soc Min Metall Explor 342(1):51–61
19. Jong EC, Luxbacher KD, Karmis ME, Westman EC (2016) Field test of a perfluoromethylcyclohexane (PMCH) permeation plug release vessel (PPRV) in an underground longwall mine. Trans Inst Min Metall Sect A Min Technol 125(2):65–70
20. Schatzel SJ, Gangrade V, Hollerich CA, Addis JD, Chasko LL (2017) Tracer gas study to determine face ventilation air and gob gas movement patterns on a bleederless longwall panel. 2017 SME Annual Meeting and Exhibit, Denver, CO, February 19–22, 2017, Pre-print 17–137

21. Jones AD, Lowrie SJ (1993) Applications of aerodynamic scale model simulations to predicting the accumulation of methane gas and airborne pollutants in modem coalmines Final report on CEC Contract 72621321229108, Edinburgh: Institute of Occupational Medicine, IOM Report TMl93108
22. Jones AD, Lowrie SJ (1994) An aerodynamic scale model for simulations of methane control at the return end of longwall retreat coalfaces. Min Eng 154(395):43–49
23. Gangrade V, Calizaya F, Nelson MG (2013) Use of a CO2 gas injection system in a laboratory model to study controlled recirculation. In Proceedings of International Association for Automation and Robotics in Construction (IAARC) August 10–14, Montreal, Canada Preprint No. 321
24. Calizaya F, Nelson MG, Bateman C, Jha A (2016) Pressure balancing techniques to control spontaneous combustion. 2016 SME Annual Conference and Expo: the future for Mining in a Data-Driven World 2016, p 261–264
25. Pan Y, Jha A, Tukkaraja P, Katzenstein K, Loring D (2019) Experimental investigation of gas dilution strategies in block cave mines. 2019 SME Annual Conference and Expo, Denver, CO, February 2019
26. Fig MK, Bogin GE Jr, Brune JF, Grubb JW (2016) Experimental and numerical investigation of methane ignition and flame propagation in cylindrical tubes ranging from 5 to 71 cm - part I: effects of scaling from laboratory to large-scale field studies. J Loss Prev Process Ind 41:241–251
27. Gangrade V, Harteis SP, Addis JD (2017) Development and applications of a scaled aerodynamic model for simulations of airflows in a longwall panel. In: proceedings of 16th North American Mine Ventilation Symposium Golden, CO: Colorado School of Mines, pp 6–17-6–24
28. Gangrade V, Harteis SP, Addis JD (2017) Studying longwall ventilation with physical modeling. Coal Age 123(6):38–39
29. Data Translation. QuickDAQ, Data logging and FFT analysis software. https://www.mccdaq.com/Products/Data-Acquisition-Software/QuickDAQ. Accessed February 2019
30. Aitken RJ, Vincent JH, Mark D (1989) Model studies to investigate the nature of air flow in mines. In: Proceedings of the Second International Symposium on Ventilation for Contaminant Control, September 20–23, London, England, Oxford, U.K: Pergamon Press, pp 327–335
31. Taylor G (1954) The dispersion of matter in turbulent flow through a pipe. Proc R Soc 223A:446–468
32. Hall DJ, Barret CF, Ralph MO (1975) Experiments on a model of an escape of heavy gas. Stevenage, Herts: Warren spring laboratory, report LR 2 17 (AP)
33. Peng SS, Chaing HS (1986) Air velocity distribution measurements on four mechanized longwall coal faces. Int J Min Geol Eng 4:235–246

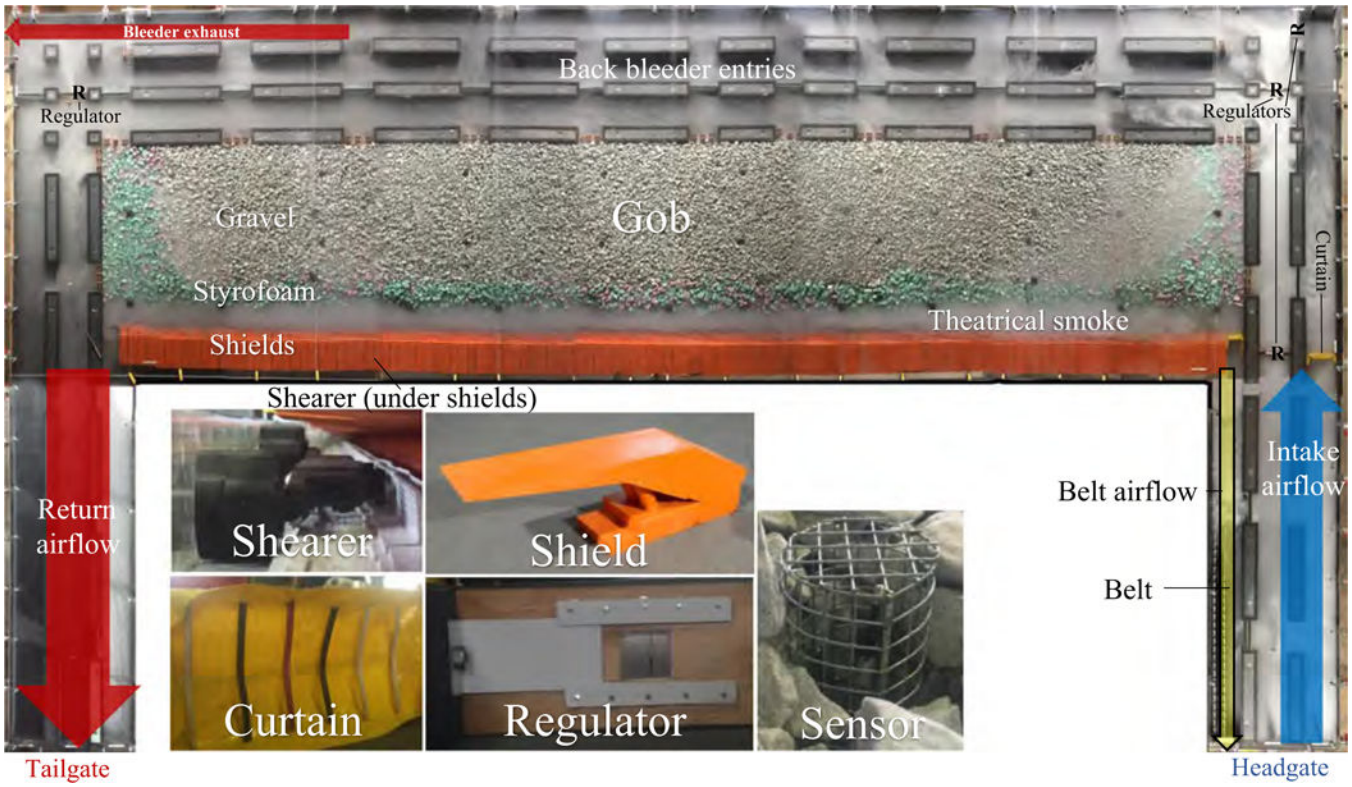

Fig. 1.
LIAM in bleeder ventilation configuration

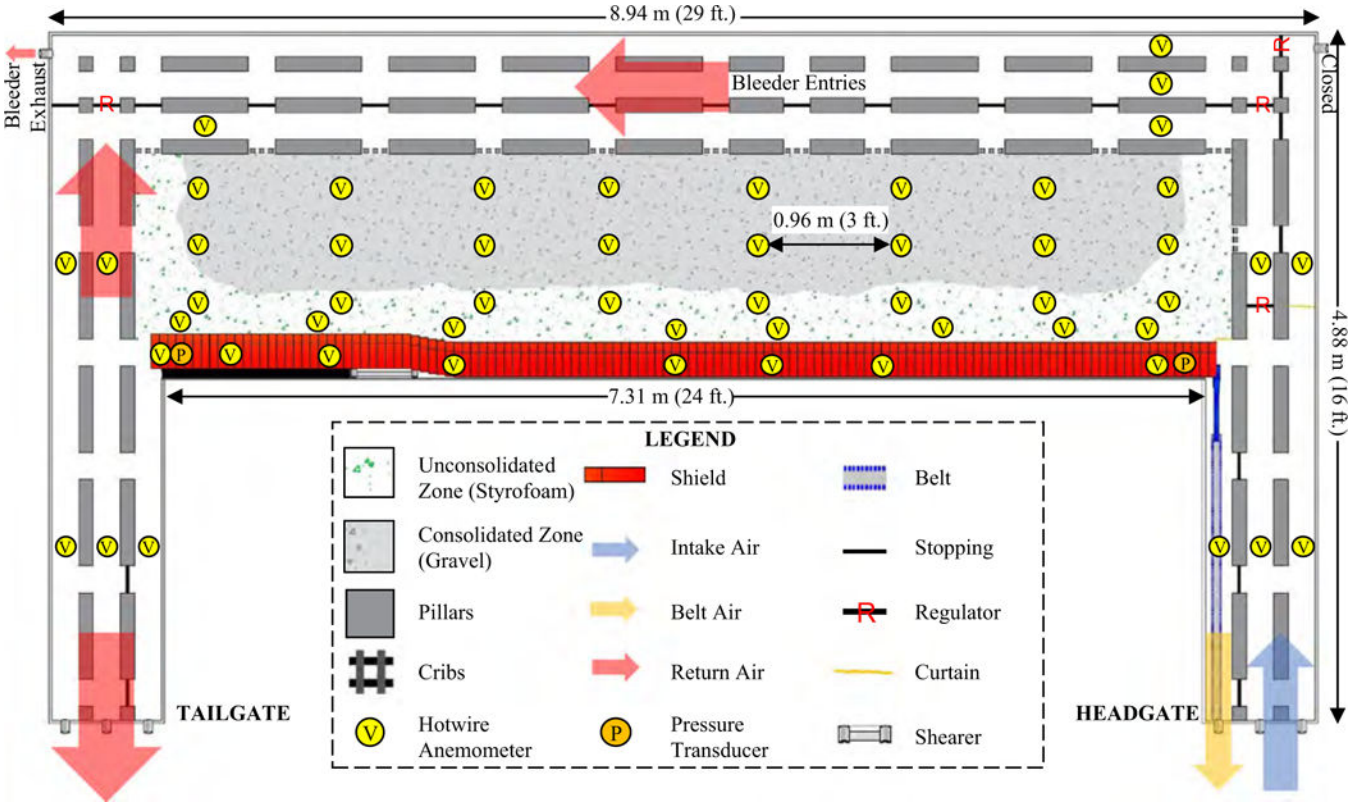

Fig. 2.
Schematic showing location of sensors, longwall features, and ventilation control

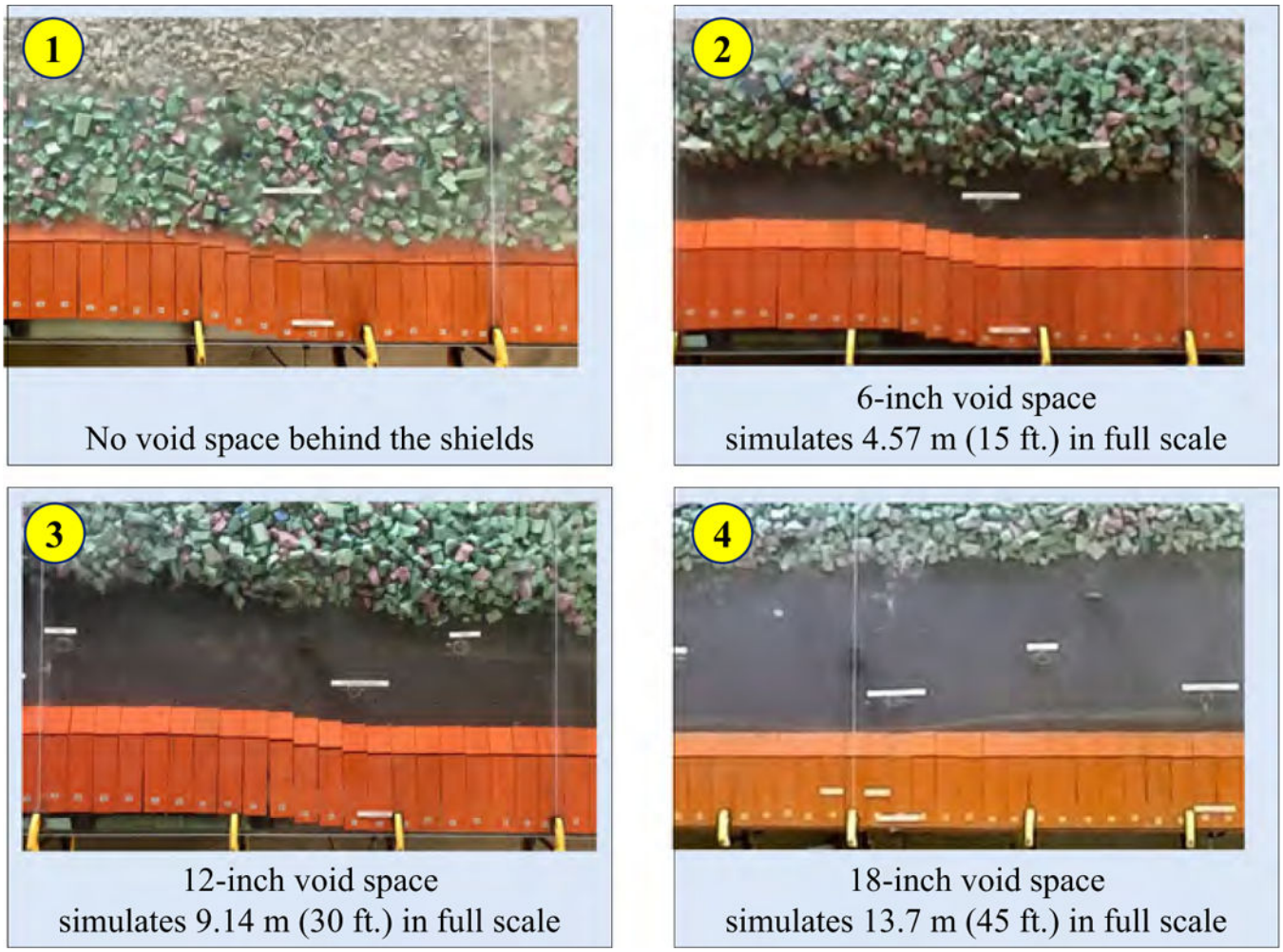

Fig. 3.
Top view near the shearer for the four caving scenarios

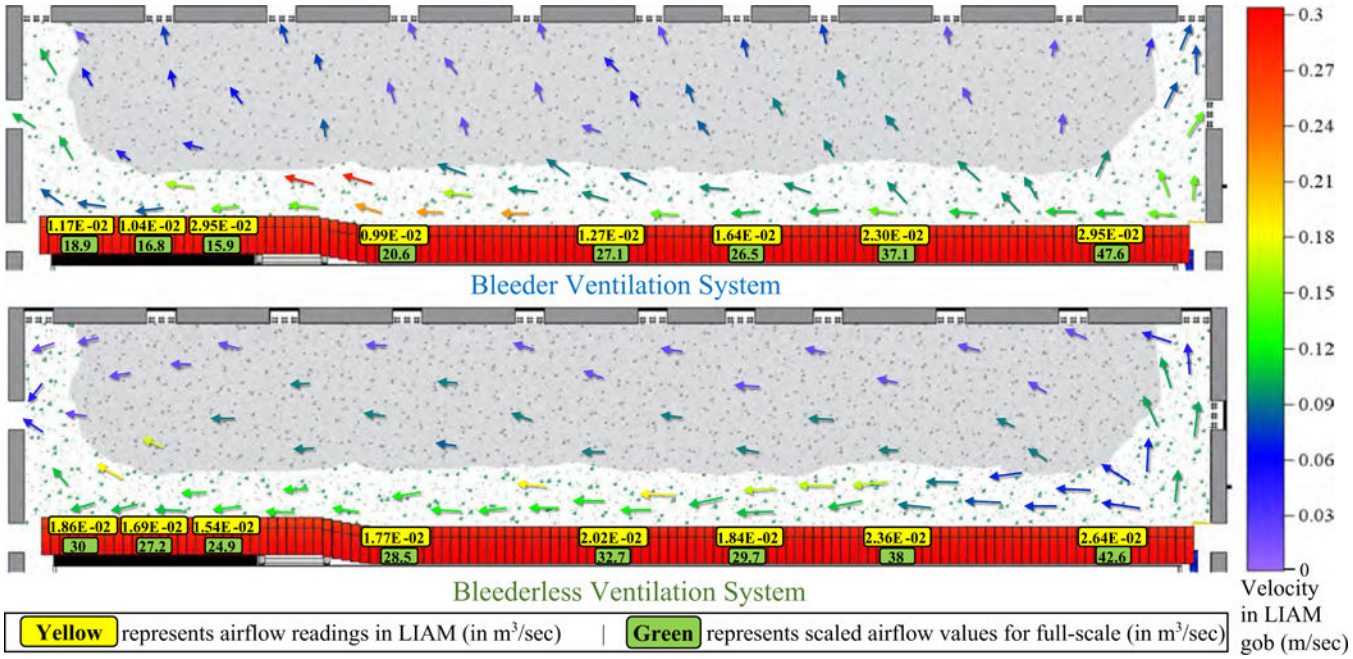

Fig. 4.

Schematic showing airflow patterns in the gob for the no void space scenario

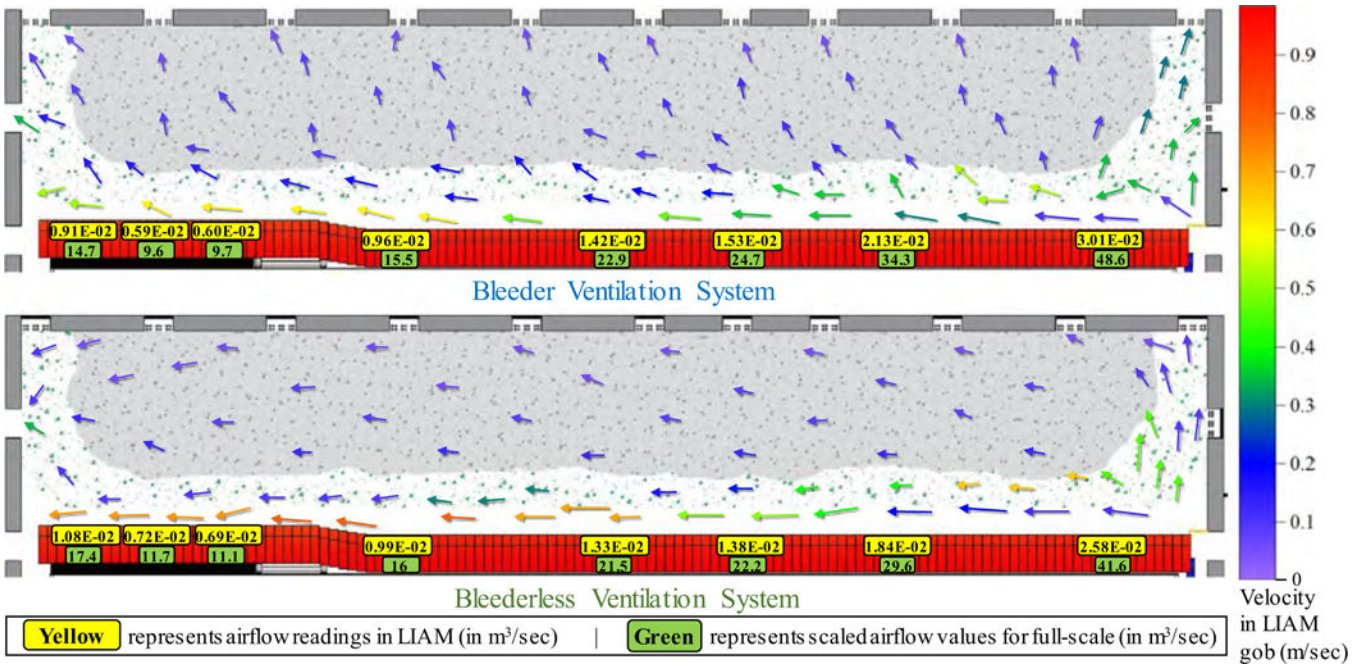

Fig. 5.
Schematic showing airflow patterns in gob for 4.57-m void space scenario

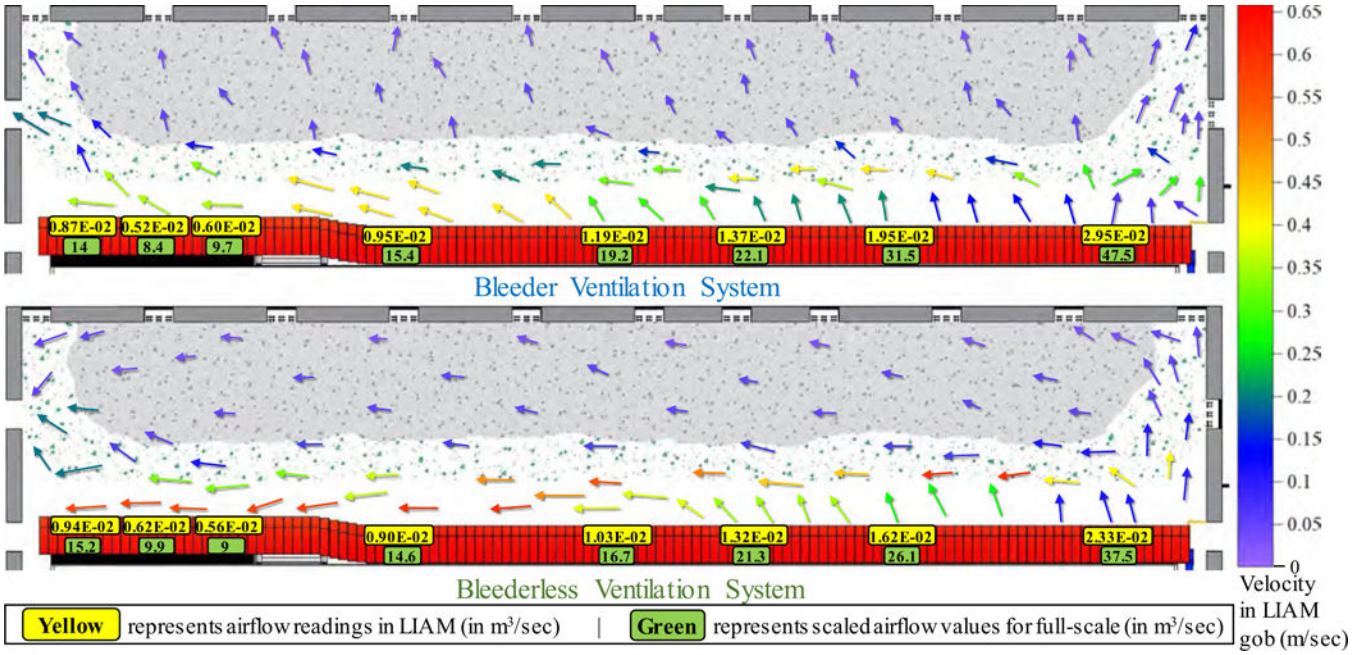

Fig. 6.

Schematic showing airflow patterns in gob for the 9.14-m void space scenario

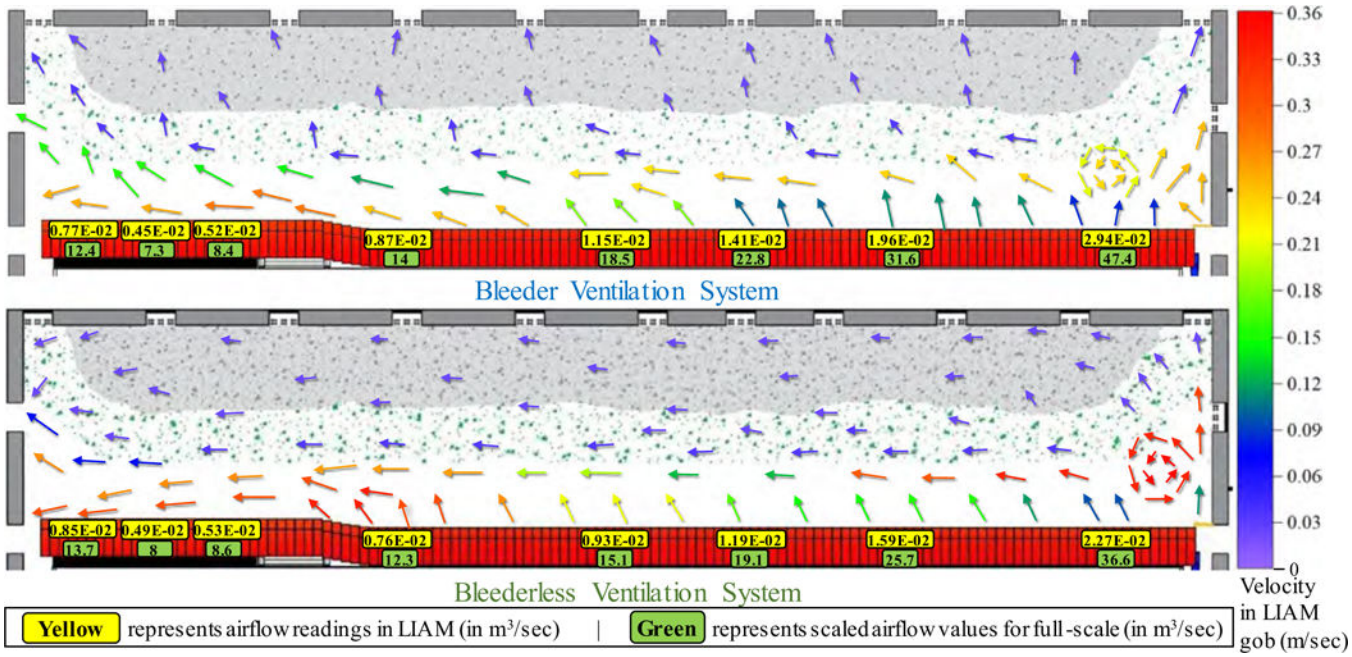

Fig. 7.

Schematic showing airflow patterns in gob for 13.7-m void space scenario

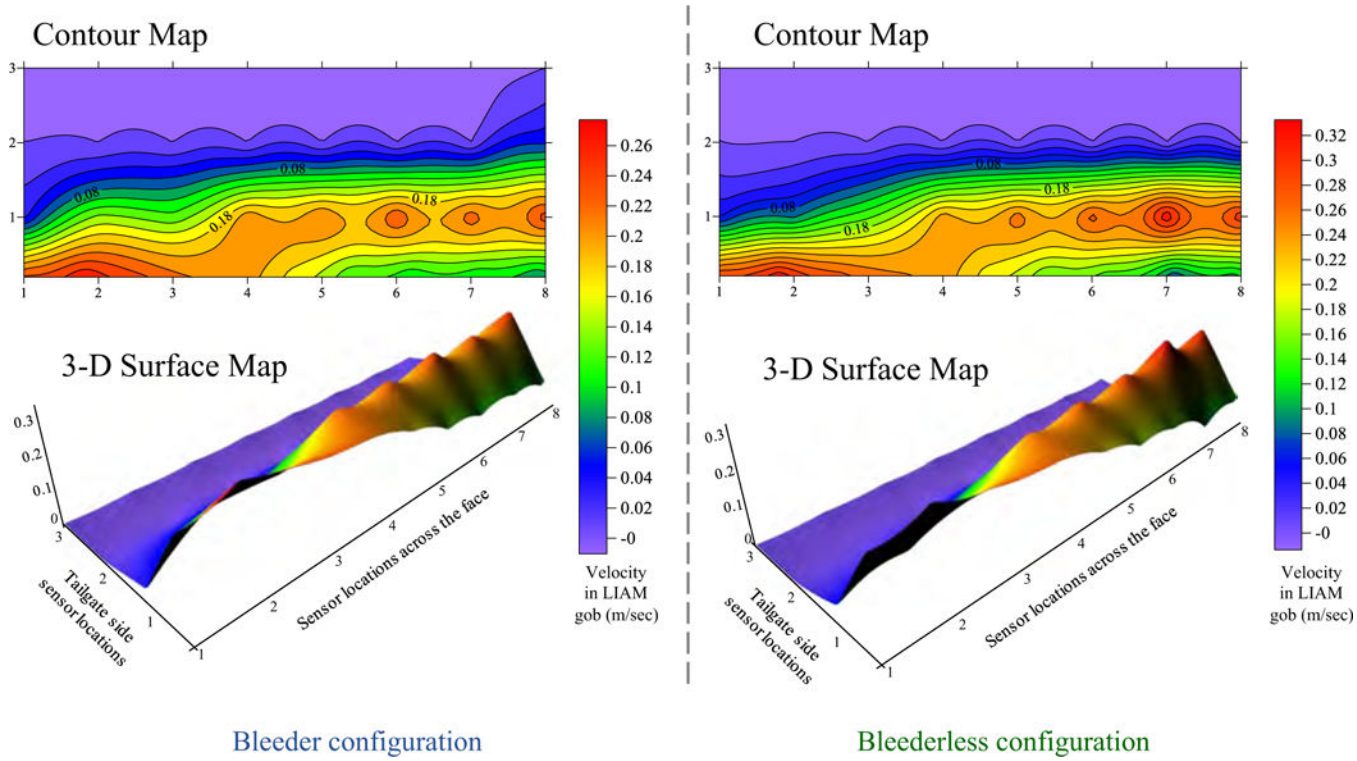

Fig. 8.

Schematic showing contour and 3-D surface map for 13.7-m void space scenario

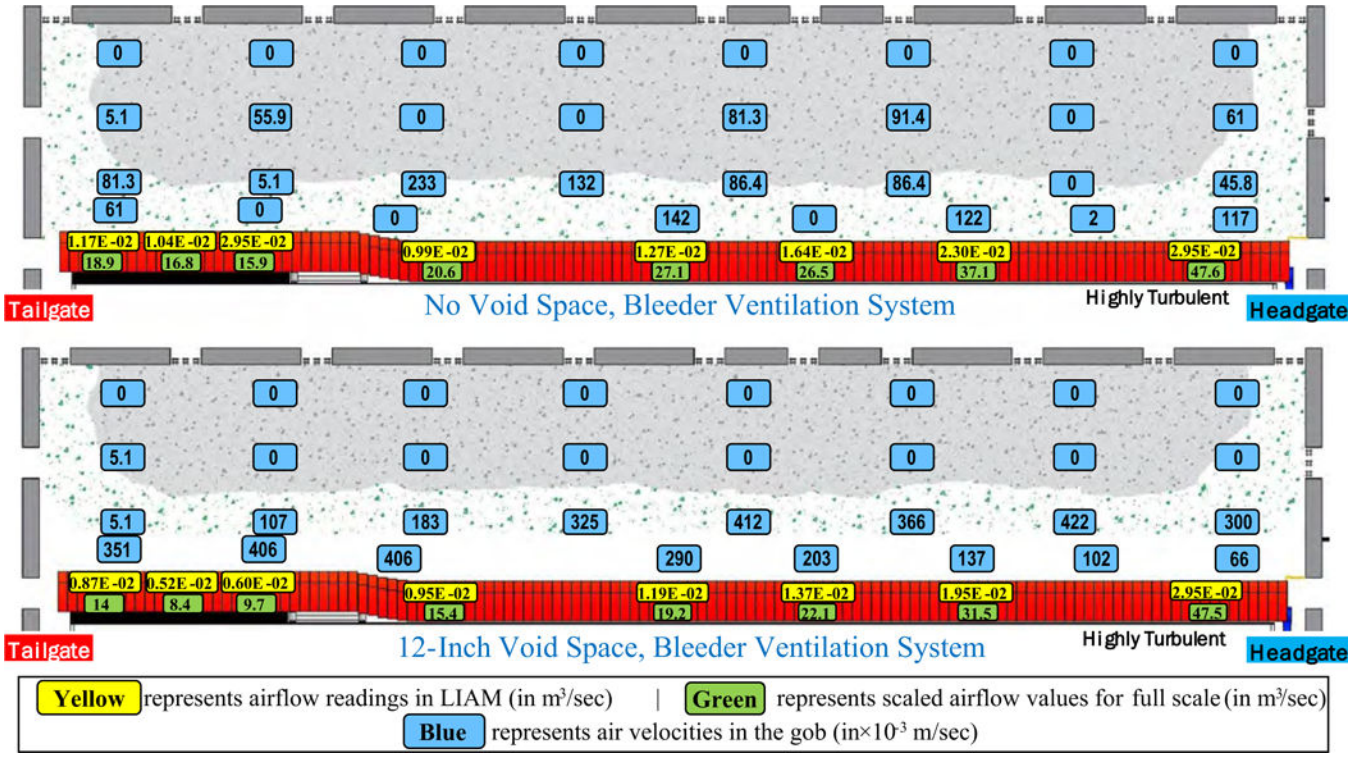

Fig. 9.

Schematic showing air velocities and scaled airflow for (a) no void and (b) 9.14-m void space caving scenarios

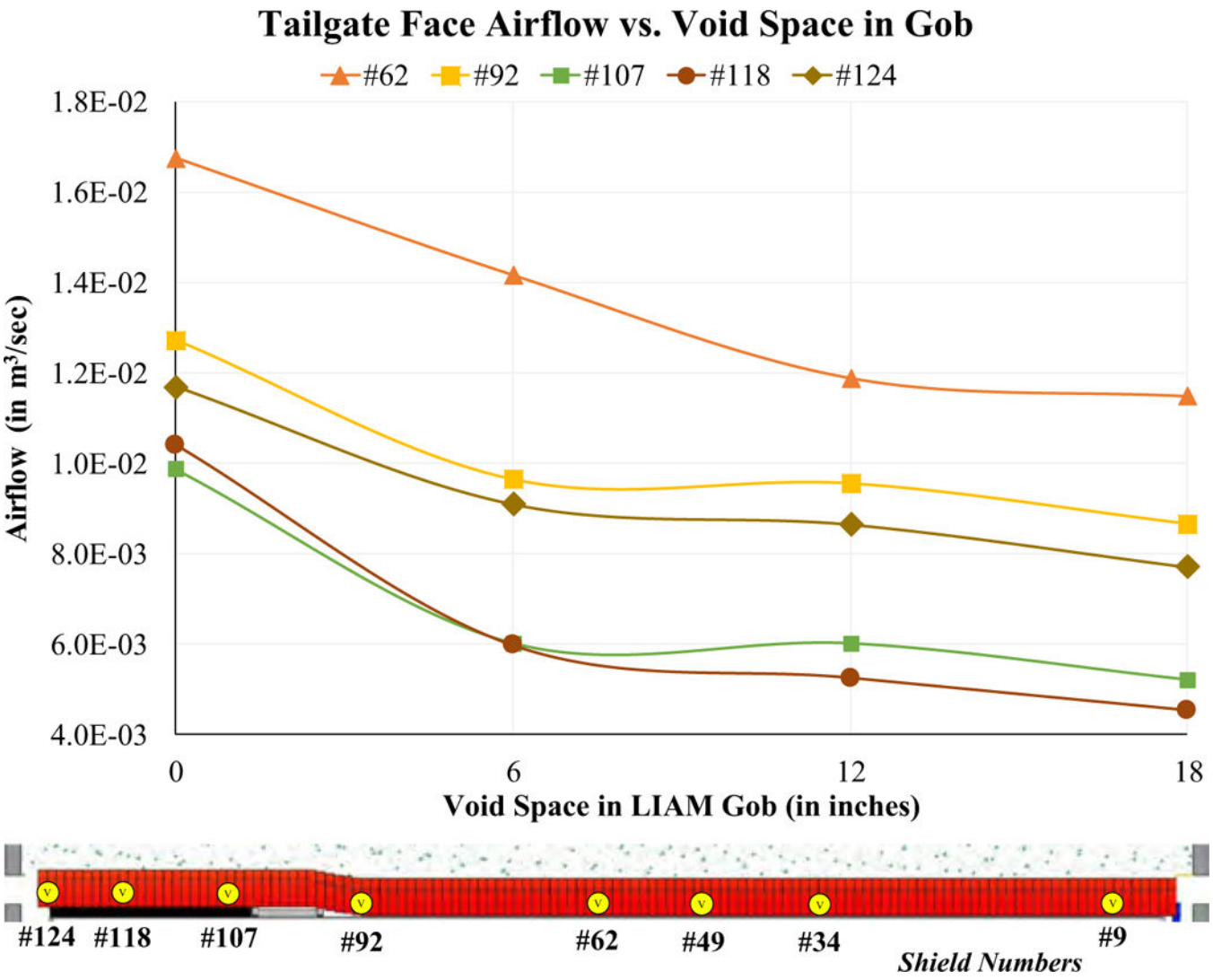

Fig. 10.

Comparison of airflow on the tailgate side of the face for different caving scenarios

Table 1

Geometrical and aerodynamic scaling factors for LIAM

Model	Specification	Characteristic
Scale for geometry	× 1/30th	7.62-cm-high face in LIAM represents 2.28-m face in full scale. 7.31-m face length in LIAM represents 219 m in full scale.
Scale for velocity	× 0.56	0.56 m/s (110 fpm) in LIAM represents 1 m/s (197 fpm) in full scale.
Scale for flow	× 6.20E-04	5.85E-02 m^3/s (124 cfm) in LIAM represents 94.4 m^3/s (200 kcfm) in full scale.
Turbulent dispersion	Reynolds number > 6000.00	Similitude for turbulent dispersion. Reynolds number ~ 12,000 in headgate entry.
Layer formation	Conservation of the Richardson number	Similitude for layering.